JNeurosci
THE JOURNAL OF NEUROSCIENCE

Research Articles: Development/Plasticity/Repair

Graded elevation of c-Jun in Schwann cells in vivo: gene dosage determines effects on development, re-myelination, tumorigenesis and hypomyelination.

Shaline V Fazal, Jose A. Gomez-Sanchez, Laura J Wagstaff, Nicolo Musner, Georg Otto, Martin Janz, Rhona Mirsky and Kristjan R Jessen

Department of Cell and Developmental Biology, University College London, Gower Street, London WC1E 6BT, United Kingdom

DOI: 10.1523/JNEUROSCI.0986-17.2017

Received: 12 April 2017

Revised: 22 September 2017

Accepted: 8 October 2017

Published: 6 November 2017

Author contributions: S.V.F., J.G.-S., L.W., and N.M. performed research; S.V.F., J.G.-S., G.O., and K.R.J. analyzed data; M.J. contributed unpublished reagents/analytic tools; R.M. and K.R.J. designed research; R.M. and K.R.J. wrote the paper.

Conflict of Interest: The authors declare no competing financial interests.

We are grateful to M Turmaine for providing help and advice for electron microscopy. This work was funded by a Wellcome Trust Programme grant to KR Jessen and R Mirsky (074665), and MRC Project grant to KR Jessen and R Mirsky (G0600967), and grant agreement No. HEALTH-F2-2008-201535 from the European Community (FP7/2007-3013).

Corresponding authors: Kristjan R Jessen, Department of Cell and Developmental Biology, University College London, Gower Street, London WC1E 6BT, United Kingdom e-mail: k.jessen@ucl.ac.uk Rhona Mirsky, Department of Cell and Developmental Biology, University College London, Gower Street, London WC1E 6BT, United Kingdom e-mail: r.mirsky@ucl.ac.uk

Cite as: J. Neurosci ; 10.1523/JNEUROSCI.0986-17.2017

Title: Graded elevation of c-Jun in Schwann cells in vivo: gene dosage determines effects on development, re-myelination, tumorigenesis and hypomyelination.

Abbreviated title: Enforced expression of c-Jun in Schwann cells

Authors: Shaline V Fazal[(1)], Jose A. Gomez-Sanchez[(1)], Laura J Wagstaff, *Nicolo Musner, **Georg Otto, ***Martin Janz, Rhona Mirsky, Kristjan R Jessen

(1) These authors contributed equally to the work

Department of Cell and Developmental Biology, University College London, Gower Street, London WC1E 6BT, United Kingdom

*Enzo Life Sciences, Inc. Industriestrasse 17, 4415 Lausen, Switzerland

**UCL Great Ormond Street Institute of Child Health, Guildford Street, London WC1N1EH, United Kingdom

***Max Delbrück Center for Molecular Medicine and Charité, University Hospital Berlin, Campus Benjamin Franklin, Robert-Roessle-Strasse 10, 13092 Berlin, Germany

Submitting author: Kristjan R. Jessen, Department of Cell and Developmental Biology, University College London, Gower Street, London WC1E 6BT, United Kingdom e-mail: k.jessen@ucl.ac.uk

Corresponding authors: Kristjan R Jessen, Department of Cell and Developmental Biology, University College London, Gower Street, London WC1E 6BT, United Kingdom e-mail: k.jessen@ucl.ac.uk Rhona Mirsky, Department of Cell and Developmental Biology, University College London, Gower Street, London WC1E 6BT, United Kingdom e-mail: r.mirsky@ucl.ac.uk

Abbreviated title: c-Jun over-expression in Schwann cells

34 pages, 9 figures,

Abstract 247, Introduction 629, Discussion 1498

The authors have no conflicts of interest to declare

Acknowledgements and funding:

We are grateful to M Turmaine for providing help and advice for electron microscopy. This work was funded by a Wellcome Trust Programme grant to KR Jessen and R Mirsky (074665), and MRC Project grant to KR Jessen and R Mirsky (G0600967), and grant agreement No. HEALTH-F2-2008-201535 from the European Community (FP7/2007-3013).

Abstract

Schwann cell c-Jun is implicated in adaptive and maladaptive functions in peripheral nerves. In injured nerves, this transcription factor promotes the repair Schwann cell phenotype and regeneration, and it promotes Schwann cell mediated neurotrophic support in models of peripheral neuropathies. However, c-Jun is associated with tumour formation in some systems, it potentially supresses myelin genes, and has been implicated in demyelinating neuropathies. To clarify these issues, and determine how c-Jun levels determine its function, we have generated, c-Jun OE/+ and c-Jun OE/OE mice, with graded expression of c-Jun in Schwann cells, and examined these lines during development, in adulthood and after injury using RNA sequencing analysis, quantitative electron microscopic morphometry, Western blotting and functional tests. Schwann cells are remarkably tolerant of elevated c-Jun, since the nerves of c-Jun OE/+ mice, where c-Jun in elevated about six fold, are normal with the exception of modestly reduced myelin thickness. The stronger elevation of c-Jun in c-Jun OE/OE mice is, however, sufficient to induce significant hypomyelination pathology, implicating c-Jun as a potential player in demyelinating neuropathies. The tumour suppressor $P19^{ARF}$ is strongly activated in the nerves of these mice, and even in aged c-Jun OE/OE mice, there is no evidence of tumours, in agreement with the fact that tumours do not form in injured nerves, although they contain proliferating Schwann cells with strikingly elevated c-Jun. Furthermore, in crushed nerves of c-Jun OE/+ mice, where c-Jun levels are over-expressed sufficiently to accelerate axonal regeneration, myelination and function are restored after injury.

Significance statement

In injured and diseased nerves, the transcription factor c-Jun in Schwann cells is elevated, and variously implicated in controlling beneficial or adverse functions, including the trophic Schwann cell support for neurons, promotion of regeneration, tumorigenesis and suppression of myelination. To analyse the functions of c-Jun, we have used transgenic mice with graded elevation of Schwann cell c-Jun. We show that high c-Jun elevation is a potential pathogenic mechanism, since it inhibits myelination. On the other hand, we do not find a link between c-Jun elevation and tumorigenesis. Modest c-Jun elevation, which is beneficial for regeneration, is well tolerated during Schwann cell development and in the adult, and is compatible with restoration of myelination and nerve function after injury.

Introduction

Schwann cell c-Jun has been implicated both in adaptive and maladaptive functions in peripheral nerves. On the one hand, in injured nerves, this transcription factor is a global amplifier of the repair Schwann cell phenotype and promotes regeneration, and in models of peripheral neuropathies Schwann cell c-Jun supports axonal survival, trophic factor expression and sensory-motor function (Arthur-Farraj et al., 2012, 2017; Hantke et al., 2014; Klein et al., 2014; Jessen and Mirsky 2016). Reduced c-Jun levels inn Schwann cells are also implicated in failure of regeneration due to ageing and long-term denervation (Painter et al., 2014; Jessen and Mirsky 2016). The c-Jun pathway is therefore of interest for the development of a pharmacology for nerve repair. On the other hand, c-Jun is associated with tumour formation in some systems, and c-Jun potentially supresses myelin genes (Eferl and Wagner 2003; Parkinson et al 2008). Based on this, it has been characterized as a negative regulator of myelination, and implicated in demyelinating neuropathies (Jessen and Mirsky 2008).

In the present work we have generated and analysed mouse lines with graded expression of c-Jun in Schwann cells in order to clarify these issues, and determine how c-Jun levels determine its function.

c-Jun is present at low levels in Schwann cells of uninjured nerves, but is rapidly elevated 80-100 fold after nerve cut (De Felipe and Hunt 1994; Shy et al., 1996; Parkinson et al., 2008; J. Gomez-Sanchez, K.R. Jessen, R. Mirsky unpublished). c-Jun elevation is also seen in human neuropathies (Hutton et al., 2011). Although c-Jun is implicated in the promotion of a number of tumours, in other situations c-Jun may have a role in the prevention of tumourigenesis by mechanisms that include activation of tumour suppressors such as $P14^{ARF}$/$p19^{ARF}$and Dmp1 (Eferl and Wagner 2003; Ameyar-Zazoua et al., 2005; Shaulian et al., 2010). $P19^{ARF}$ is elevated in Schwann cells after nerve transection, and the striking activation of Schwann cell c-Jun after injury is not associated with tumour formation (Gomez-Sanchez et al., 2013; Jessen et al., 2015b). Rather, the role of c-Jun is to take part in controlling the conversion of myelin and Remak cells to Schwann cell specialized to carry out injury-specific tasks and promote repair (Jessen et al., 2015a; Jessen and Mirsky 2016; Arthur-Farraj et al., 2017). This includes preventing the death of injured neurons and promoting axon growth by expression of trophic factors, guiding axons back to their targets by forming regeneration tracks (Bungner bands), and breakdown of myelin directly by autophagy and indirectly by cytokine expression to recruit macrophages. Inactivation of Schwann cell c-Jun results in defective repair Schwann cells and impaired regeneration (Arthur-Farraj et al., 2012; Jessen and Mirsky 2016).

The injury-induced extinction of myelin genes is also delayed without c-Jun, indicating that c-Jun has a dual function, promoting the expression of the repair phenotype and the suppression of the myelin phenotype. c-Jun suppression of myelin genes has only been studied directly in culture, where c-Jun suppresses the Krox20- or cAMP-induced activation of myelin genes, and enforced c-Jun inhibits myelination in co-cultures (Parkinson et al., 2004; 2008). Negative transcriptional regulation of myelination has also been shown for Notch1 and Sox2 in vivo and suggested for other factors including Pax-3, Id2 and Sox-2 based on cell culture experiments (Jessen and Mirsky 2008; Roberts et al., 2017).

The present results show that the function of c-Jun in Schwann cells depends on gene dosage, and that Schwann cells are surprisingly tolerant of the moderately (~ 6-fold) elevated c-Jun, seen in c-Jun OE/+ mice. In these mice, where over-expression of c-Jun is sufficient to accelerate axonal regeneration (Wagstaff et al., 2017), myelination and function are restored after nerve injury. Further, even high expression of c-Jun is not associated with tumour formation in Schwann cells, although this is sufficient to cause hypo-myelination neuropathy.

Materials and methods

Transgenic mice

Animal experiments conformed to UK Home Office guidelines under the supervision of UCL Biological Services. To generate mice that overexpress c-Jun selectively in Schwann cells, female *R26c-Junstopf* mice, generated in the laboratory of Klaus Rajewsky, which carry a lox-P flanked STOP cassette in front of a CAG promoter driven c-Jun cDNA in the ROSA26 locus, were crossed with male *P0Cre*$^{+/-}$ mice (Feltri et al., 1999). This generated *P0-Cre*$^{+/-}$*;R26c-Junstopf*$^{f/+}$ mice, which we refer to as c-Jun OE/+ mice. These male mice were back-crossed with female *R26c-Junstopf*$^{f/f}$ mice to generate *P0-Cre*$^{+}$*;R26c-Junstopf*$^{f/f}$ mice, referred to as c-Jun OE/OE mice. *P0-Cre*$^{-/-}$ littermates were used as controls. Mice of either sex were used in the experiments. The mice are on the C57BL/6 background.

Genotyping

DNA for genotyping was extracted from ear or tail samples using the HotSHot method (Truett et al., 2000). Primers for genotyping the R26c-Junstopf transgene were 5'-TGGCACAGCTTAAGCAGAAA-3' and 5'-GCAATATGGTGGAAAATAAC-3' (270bp). The primers for the Rosa26 wildtype locus were 5'GGAGTGTTGCAATACCTTTCTGGGAGTTC-

3' and 5'TGTCCCTCCAATTTTACACCTGTTCAATTC-3' (217bp band). The primers for the P0-Cre transgene were 5'-GCTGGCCCAAATGTTGCTGG-3' and 5'CCACCACCTCTCCATTGCAC-3' (480bp band).

Nerve injury

The sciatic nerve was exposed and crushed (3x15 sec at three rotation angles) at the sciatic notch using angled forceps. The wound was closed using veterinary autoclips. The nerve distal to the crush was excised for analysis at various time points. Contralateral uninjured sciatic nerves were used as controls for western blotting, immunofluorescence or electron microscopy.

Schwann cell culture

Schwann cell cultures were prepared from sciatic nerves of postnatal day 8-10 mouse pups essentially as in Morgan et al., (1991) and Arthur-Farraj et al., (2011). After enzymatic dissociation and centrifugation, the cell pellet was resuspended in defined medium (DM) (Meier et al., 1999), containing 10^{-6} M insulin and 5% HS, and plated in drops on coverslips coated with Poly-L-lysine and laminin. Cells were incubated at 37°C/5%CO2 and allowed to adhere for 24 hr. After 24 hr, the medium was changed to DM/0.5% HS (controls), or DM with 10ng/ml NRG1 alone, or DM with NRG1 10ng/ml and dbcAMP 1mM for 48 hr before fixation and immunolabelling.

Antibodies

The following antibodies were used for Immunofluorescence: c-Jun (Cell Signalling, rabbit 1:800, 9165), Ki67 (Abcam, rabbit 1:100, ab15580), Krox20 (Covance, rabbit 1:100, PRB-236P), SOX-10 (R&D Systems, goat 1:100, AF2864), donkey anti-goat IgG (H+L) Alexa Fluor 488 conjugate (Molecular Probes, 1:1000, A11057), Cy3 donkey anti-rabbit IgG (H+L) (Jackson Immunoresearch, 1:500, 711-165-152), biotinylated anti-rabbit IgG (Amersham, 1:600, RPN1004), Cy3 Streptavidin (Jackson Imunnoresearch, 1:500, 016-160-084).

The following antibodies were used for Western blot: GAPDH (Sigma, rabbit 1:5000, G9545), Calnexin (Enzo Life Sciences, rabbit 1:1000, ADI-SPA-860-D), c-Jun (Cell Signalling, rabbit 1:1000, 9165), Krox20 (Millipore, rabbit 1:500, ABE1374) , Mpz (AvesLab, chick 1:2000, PZO), cyclin D1 (Santa Cruz, rabbit 1:200, sc-450), p19 Arf (5-c3-1) (Santa

Cruz, rat 1:100, sc-32748), anti-mouse IgG HRP-linked (Promega, 1:2000, W4028), anti-rabbit IgG, HRP-linked (Cell Signaling, 1:2000, 7074), anti-rat IgG, HRP-linked (Cell Signaling, 1:2000, 7077) anti-chicken IgY, HRP-linked (Promega, 1:2000, G1351).

Immunohistochemistry

Schwann cells were fixed in 4% paraformaldehyde/PBS for 15 min and then immunolabelled. Transverse sciatic nerve cryosections (10µm) were post fixed with 4% paraformaldehyde/PBS for 15 min, blocked in 0.2%Triton-X-100, 10%HS in PBS and subsequently incubated with primary antibodies in blocking solution overnight at 4ºC, followed by 2 hr in secondary antibodies and DAPI to identify cell nuclei (Thermofisher, 1:50000). For Ki67 staining biotin antibodies followed by Cy3 Streptavidin were used.

Western Blotting

For blotting, homogenates were obtained from injured and uninjured nerves as well as cultured nerve segments essentially as described previously (Gomez-Sanchez et al., 2015). Experiments were repeated at least three times with fresh samples and representative pictures are shown. Densitometric quantification was by Image Lab 4.1 (Bio-Rad Laboratories). Measurements were normalized to loading control GAPDH and/or calnexin.

RNA sequencing analysis

Library preparation: Total RNA was isolated using the RNeasy Lipid Tissue Mini Kit (Qiagen) with a DNase I step performed to eliminate traces of genomic DNA.The purified mRNA was fragmented, and primed with random hexamers. Strand-specific first strand cDNA was generated using Reverse Transcriptase in the presence of Actinomycin D. The second cDNA strand was synthesised using dUTP in place of dTTP, to mark the second strand. The resultant cDNA was then “A-tailed” at the 3’ end to prevent self-ligation and adapter dimerisation. Truncated adaptors, containing a T overhang were ligated to the A-Tailed cDNA. Successfully ligated cDNA molecules were then enriched with limited cycle PCR (10-14 cycles. The high fidelity polymerase used in the PCR is unable to extend through uracil. This means only the first strand is amplified for sequencing, thus making the library strand specific.

Sequencing: Libraries to be multiplexed in the same run were pooled in equimolar quantities. Samples were sequenced on the NextSeq 500 instrument (Illumina, San Diego, US) resulting in ~ 16M reads per sample.

Data Analysis: Run data were demultiplexed and converted to fastq files using Illumina's bcl2fastq Conversion Software v2.18 on BaseSpace. Fastq files were aligned to a reference genome using STAR on the BaseSpace RNA-Seq alignment app v1.1.0. Reads per transcript were counted using HTSeq and differential expression was estimated using the BioConductor package DESeq2 (BaseSpace app v1.0.0).

The RNA Sequencing analysis was carried out by UCL Genomics, UCL Great Ormond Street Institute of Child Health

Electron microscopy

Nerves were processed as previously described (Gomez-Sanchez et al., 2015). Transverse ultrathin sections from neonatal, P7 and P21 sciatic nerve or adult (P60) or aged (P300) sciatic nerve, or from injured distal stumps of adult sciatic nerves were taken 5 mm from the sciatic notch or cut site and mounted on film.

Photographs were taken using a Jeol 1010 electron microscope with Gatan camera and software. Images were analysed using NIH ImageJ. Photographs at were taken at 3000x to measure the number of myelinated axons, non-myelinated axons bigger than 1.5μm and Schwann cell nuclei. The nerve area was measured from photographs taken at 200x magnification. Higher magnifications were used to show the Remak bundles or any abnormal morphology found in the nerve.

The percentage of extracellular matrix was analysed using ImageJ software by converting electron microscopy images at 5000x and 10000x into 8-bit images and tracing the presence of extracellular matrix.

Behavioural Tests

Experiments conformed to UK Home Office guidelines. Nine or more mice/ genotype were tested. Six week old mice were tested before surgery to ensure that there were no differences in normal responses between the genetic backgrounds. Sciatic function index (Inserra et al., 1998), toe spread reflex (Ma et al.,2011) and the toe pinch test, modified from Collier et al., (1961), were carried out as in Arthur-Farraj et al., (2012).

254

255 Statistical Analysis

256 Results are expressed as mean ± SEM. Statistical significance was estimated by one-way
257 ANOVA with Tukey correction, two-way ANOVA with Bonferroni's multiple comparison,
258 Mann-Whitney U-test, or Student`s T-test. A P value < 0.05 was considered as statistically
259 significant. Statistical analysis was performed using GraphPad software (version 6.0).

260

261 **Results**

262 **Adult uninjured nerves of c-Jun OE/+ and c-Jun OE/OE mice have high levels of c-Jun**
263 **protein in Schwann cell nuclei**

264 Diagrammatic representation of how the c-Jun overexpressing mice were bred and produced
265 is shown in Fig. 1A. The *R26c-Junstopf* mouse has a c-Jun cDNA insert in the Rosa26 WT
266 locus with two flanking loxP sites either side of a STOP codon. These mice were bred with
267 *P0Cre*$^{+/-}$ mice (Feltri et al., 1999). In the presence of Cre recombinase, the STOP codon is
268 removed and c-Jun is overexpressed specifically in Schwann cells (Feltri et al., 1999).
269 *P0Cre*$^{-/-}$*;R26c-Junstopf*$^{f/+}$ control mice will be referred to as WT, while *P0Cre*$^{+/-}$*; R26c-*
270 *Junstopf*$^{f/+}$ will be referred to as c-Jun OE/+ mice, and *P0Cre*$^{+/-}$*; R26c-Junstopf*$^{f/f}$ will be
271 referred to as c-Jun OE/OE. Genotyping of WT, c-Jun OE/+ and c-Jun OE/OE mice is shown
272 in Fig. 1B.

273 We examined c-Jun protein expression in adult (postnatal day (P) 60) uninjured sciatic
274 nerves of c-Jun OE/+ and c-Jun OE/OE mice and compared this with that seen in WT mice.
275 Double immunolabelling with c-Jun antibodies and Sox10 antibodies to specifically identify
276 Schwann cell nuclei showed that Schwann cells in c-Jun OE/+ nerves expressed clearly
277 elevated nuclear c-Jun levels compared to that seen in WT nerves, which showed barely
278 detectable c-Jun using this staining protocol (see Materials and Methods). In c-Jun OE/OE
279 nerves, nuclear c-Jun levels were further increased (Fig. 1C). No increase in c-Jun was seen
280 in Sox10 negative nuclei, labelled with DAPI (not shown), indicating that c-Jun over
281 expression in these mouse lines was Schwann cell specific in agreement with previous
282 observations (Feltri et al., 1999).

283 Western blotting showed that c-Jun protein levels in uninjured adult sciatic nerves were
284 elevated about six fold in c-Jun OE/+ mice and about 28 fold in c-Jun OE/OE mice,
285 compared to WT (Fig. 1D). In c-Jun OE/+ mice, c-Jun mRNA levels were 4.5 fold higher than
286 in WT nerves.

These data indicate that the axonal signals that normally suppress c-Jun during myelination in vivo fail to supress c-Jun expression from the c-Jun OE transgene, as expected (Parkinson et al., 2008; Jessen and Mirsky 2008). We verified this by exposing purified Schwann cell cultures to signals that mimic axonal myelin signals in mice, namely the combined activation of cAMP and neuregulin pathways (Arthur-Farraj et al., 2011). In these experiments, a combination of 1 mM dbcAMP and 10nM neuregulin failed to suppress nuclear c-Jun expression in c-Jun OE/+ cells although down-regulation of c-Jun protein was seen in WT cells (Fig. 1E).

The elevation of c-Jun specifically in Schwann cell nuclei in c-Jun OE/+ and c-Jun OE/OE mice allowed us to study in vivo the effects of a graded increase in c-Jun expression on Schwann cells in uninjured and injured nerves.

Transcriptional profiling of uninjured nerves in WT, c-Jun OE/+ and c-Jun OE/OE mice

To document changes in gene expression caused by c-Jun elevation in c-Jun OE/+ and OE/OE mice, we carried out RNA sequencing analysis on uninjured adult (P60) sciatic nerves. Heat map and Principal Component Analysis (PCA) confirmed that c-Jun overexpression was the dominant source of differential gene expression (Fig.2 A,B). In OE/+ nerves, which express about six fold WT levels of c-Jun protein, 67 genes were ≥2 fold up-regulated and 25 genes were ≥2 fold down-regulated compared to WT nerves. Among 13 genes we considered of particular interest, one gene was regulated ≥2 fold. This was *Shh* which was up-regulated (Fig. 2C). *c-Jun* was expressed at 153% of WT levels, and GDNF at 182% of WT levels, while the myelin protein genes *Mbp* and *Mpz* were expressed at about 65% and 75% of WT levels, respectively. Notably, the mRNA level for *Krox20 (Egr2),* a key myelin regulator, was essentially unchanged. The 15 most up- and down-regulated genes in c-Jun OE/+ are shown in Fig. 3A.

In OE/OE nerves, which express about 28 fold WT levels of c-Jun protein, 909 genes were ≥2 fold up-regulated and 1055 genes were down-regulated by ≥2 fold compared to WT nerves. Most of the 13 genes of particular interest changed expression by ≥2 fold in these mice (Fig. 2C) .This included *c-Jun*, which was elevated four-to-five fold, *Gdnf,* which was elevated by about 56 fold, and *Shh* and *Olig1*, which were elevated 20 fold and 48 fold respectively. The myelin protein genes *Mbp* and *Mpz*, were reduced to 13-14 % of WT levels. The 15 most up- and down-regulated genes in c-Jun OE/OE nerves are shown in Fig. 3B.

A comparison of gene expression between OE/+ and OE/OE mice with respect to the 13 genes of interest and the most regulated genes is shown in Figs. 2C and 3C respectively.

The fact that in both c-Jun OE/+ and OE/OE mice, c-Jun protein was more strongly elevated, in terms of fold change from WT, than c-Jun mRNA, suggests that posttranscriptional controls are important in controlling c-Jun levels.

Expression of myelin-related proteins in uninjured nerves of OE/+ and OE/OE mice

We examined two key myelin related proteins, the pro-myelin transcription factor Krox20 (Egr2) and the myelin adhesion protein Pzero (Mpz) in uninjured sciatic nerves of c-Jun OE/- and OE/OE mice. In line with the mRNA data, Krox20 levels were essentially unaffected in c-Jun OE/+ mice, both in double label immunohistochemical experiments, which show Krox20 in Schwann cell nuclei, and in Western blotting experiments (Fig. 3D,E). Mpz levels in these mice were about 15 % lower than those found in WT mice (Fig. 3F). In contrast, the c-Jun OE/OE mice expressed significantly less Krox20 protein in Schwann cell nuclei and Western blots (Fig. 3D,E), and much reduced levels of Mpz (Fig. 3F).

This indicates that in adult-Jun OE/+ nerves, the levels of key myelin-related proteins and their mRNA remain relatively mildly affected**,** in spite of about six fold elevation of Schwann cell c-Jun. This tolerance does, however, break down when c-Jun levels are elevated about 28 fold as seen in c-Jun OE/OE mice, in line with the capacity of c-Jun to negatively regulate myelin genes indicated in experiments in vitro and in mice with conditional inactivation of Schwann cell c-Jun (Parkinson et al., 2004; 2008; Arthur-Farraj et al., 2012).

Structure of adult nerves is nearly normal in c-Jun OE/+ mice

Although the levels of myelin proteins were normal in c-Jun OE/+ mice, it remained possible that the substantial c-Jun elevation affected myelination and nerve architecture. This was tested by a morphometric comparison of WT and c-Jun OE/+ nerves.

The general appearance of WT and c-Jun OE/+ nerves of 60 day old mice was similar (Fig. 4A). The size of the cross-sectional profiles of the sciatic nerve and the number of Schwann cell nuclei were not significantly different between the two genotypes, and Ki67 labelling of Sox10 positive cells failed to show significant increase in Schwann cell proliferation (Fig 4B-D). WT and c-Jun OE/+ nerves had similar numbers of >1.5 μm axons per nerve profile, and the percentage of segregated (1:1), myelin-competent (>1.5μm diameter) axons that were myelinated, and the total number of myelinated axons were comparable (Fig 4E-G). Both WT and c-Jun OE/+ nerves contained similar very low numbers of myelin-competent (>1.5 μm diameter) axons in a 1:1 relationship that remained unmyelinated (Fig. 4H). Measurements of g-ratios showed that myelin sheaths were slightly thinner in c-Jun OE/+

354 mice compared to WT (Fig. 4I). Remak bundles in c-Jun OE/+ mice appeared normal, and
355 the percentage of >1.5μm axons that were found within Remak bundles was similar and very
356 low in both genotypes (Fig. 4J).

357 We found that this similarity between WT and c-Jun over-expressing c-Jun OE/+ 60 day old
358 mice remained even in old (300 day) mice (Fig. 4K-S). As in young mice, observations of
359 general appearance and quantitative analysis failed to reveal significant differences between
360 the two genotypes, except for the difference in G-ratios, a difference that was also seen in
361 young mice (Fig. 4R). The only age-induced change related to Schwann cell numbers, which
362 were somewhat elevated in old mice, the difference between the genotypes reaching
363 statistical significance (Fig. 4M).

364 These observations show that although c-Jun OE/+ mice show about six fold elevation of c-
365 Jun protein that is localized to Schwann cell nuclei, they achieve essentially normal
366 Schwann cell and nerve architecture, with the exception of modestly reduced myelin
367 thickness.

368 **Adult nerves of c-Jun OE/OE mice are hypomyelinated, show onion bulbs and hyperplasia**

369 **but do not form tumours**

370 In contrast to c-Jun OE/+ mice, the higher (about 28 fold) c-Jun expression c-Jun OE/OE
371 mice resulted in obvious lack of myelin in 60 day old mice (Fig. 5A). Although the total
372 number >1.5μm axons was similar to WT (Fig. 5B), the percentage of segregated (1:1),
373 myelin-competent (>1.5 μm diameter) axons that were myelinated was reduced by about
374 40% (Fig. 5C), and there was a corresponding increase in the number of myelin-competent
375 axons that that had reached a 1:1 relationship but remained unmyelinated (Fig. 5E). The
376 myelin sheaths in c-Jun OE/OE mice were also thin compared to WT (Fig. 5F). While all of
377 this indicates impediment to myelination, a sorting defect was indicated by the fact that the
378 percentage of >1.5 μm axons that remained within Remak bundles was strikingly increased
379 to about 28% compared to <1% in WT (Fig. 5G). As a result of impaired myelination and
380 sorting, the number of myelinated axons in c-Jun OE/OE nerves was substantially lower than
381 in WT nerves (Fig.5D). As seen in mouse models of CMT1A neuropathy and a number of
382 other mouse mutants with elevated, non-tumorigenic Schwann cell proliferation, the
383 organization of Remak bundles was somewhat altered (Robertson et al., 2002; Chen et al.,
384 2003; Ling et al., 2005; Verhamme et al., 2011). The cells sometimes showed increased
385 membranous structures and processes that were not in contact with axons, and they
386 contained fewer axons per transverse section of a bundle, suggesting the presence of a
387 larger number of Remak cells each taking care of fewer axons (Fig 5A). Increased mast cell

numbers are seen in several neuropathic conditions and mutant models and after mechanical nerve injury (Olson 1971; Ling et al. 2005; Ishii et al. 2016). We therefore counted mast cell numbers and found substantial elevation in c-Jun OE/OE nerves (Fig. 5H).

An increase in Schwann cell number, a feature of many neuropathies including CMT1A (Robertson et al., 2002; Lupski and Chance 2005) , was also seen in c-Jun OE/OE nerves, the total number of Schwann cell nuclei per nerve profile being about six fold that in WT (Fig. 5I). Western blots of Cyclin D1 indicated ongoing proliferation among the cells of c-Jun OE/OE nerves (Fig. 5J). Proliferation of Schwann cells was indicated in double immunolabelling with Ki67 and Sox10 antibodies to detect dividing Schwann cells, since double labelled Schwann cells, although few, were about three times more common in c-Jun OE/OE nerves than in WT nerves (Fig. 5K). Observations in the electron microscope provided no evidence for the presence of a significant number of Schwann cells without contact with axons. The increased number of Schwann cell nuclei in nerve sections is likely due to non-myelinating cells in a 1:1 ratio with axons being shorter than myelin cells, cells with thin myelin sheaths being shorter than those with normal sheath thickness, and increased number of Remak cells.

The sciatic nerves of 60 day old c-Jun OE/OE mice were enlarged, showing total cross-sectional profiles that were about twice that in c-Jun OE/+ or WT nerves (Fig. 5L). Collagen containing extracellular space was also markedly increased in c-Jun OE/OE nerves, occupying 133,349 μm^2 (+/-19,891; n=3) (54% of nerve area) in 60 day c-Jun OE/OE nerves, but only 16,069 μm^2 (+/-2,834; n=5) (13% of nerve area) in WT nerves (Fig. 4M)**.** This amounts to an increase in extracellular space of 116,280 μm^2 . Since the nerves of c-Jun OE/OE nerves are 121,486 μm^2 larger than WT nerves, more that 95% of the enlargement seen in c-Jun OE/OE nerves is due to increased collagen-containing extracellular space, with a likely contribution from increased number of Remak cells and cells other than Schwann cells. Increase in endoneurial connective tissue is seen in a number of neuropathies including CMT1A, and in the *trembler* and *twitcher* mouse mutants (Palumbo et al., 2002; Fledrich et al., 2012; Low 1977; Ling et al. 2005; Kagitani-Shimono 2008).

We examined the mutant nerves extensively for the presence tumours or cellular arrangements reminiscent of tumour formation, but failed to find any evidence in this direction. In line with this, the tumour suppressor $p19^{ARF}$ was strongly elevated in uninjured nerves of c-Jun OE/EO mice (Fig. 5N).

Examination of old (P300) mice showed that only three of the parameters studied above changed obviously with age. (Fig. 6A-J). This was the appearance of significant numbers of

onion bulbs (Fig. 6F,G), reduction in Schwann cell proliferation, which was no longer significantly elevated (Fig. 6J), and a reduction in the percentage of >1.5 μm axons that remained within Remak bundles, from about 28% at P60 (Fig. 5G) to less than 2% (Fig. 6E). Thus, in nerves of c-Jun OE/OE mice, a large number of axons appear to gradually segregate from Remak bundles between P60 and P300. The proportion of these >1.5 μm axons that myelinate is similar to that of the >1.5 μm segregated axons in P60 nerves, or about 60% (Fig. 6B). No tumours were found in older mice (n=18).

Developmental myelination is delayed in c-Jun OE/+ mice, but inhibited in c-Jun OE/OE mice

Although adult nerves of c-Jun OE/- mice are essentially normal, we tested whether the c-Jun elevation in these nerves caused a delay in myelination during development. We also determined whether the lack of myelin in the adult c-Jun OE/OE nerves was due to de-myelination in the adult or inhibition of myelination during development.

In developing nerves of c-Jun OE/+ mice, there was a trend towards c-Jun elevation at P1, but this was not significant, while at P7 Jun was elevated about six fold compared to WT nerves at the same age. This failed to suppress levels of the myelin proteins Mpz and Krox20 in Western blots (Fig. 7A,B). But nuclear Krox20 was reduced, judged by double labelling of nerve sections with Krox20 and Sox10 antibodies to identify Schwann cells (Fig.7 C).

In developing nerves of c-Jun OE/OE mice, c-Jun levels at P7 were about eight fold that found in WT mice at that age, and Mpz was suppressed in Western blots (Fig. 7A). Although Krox20 levels were not significantly reduced in Westerns, the number of Schwann cells that showed nuclear Krox20 was less 50% of that in WT nerves, as seen in double immunolabeling of nerve sections Fig. 7B,C).

Electron microscopy at P1, P7 and P21 showed that in c-Jun OE/+ mice, myelination was transiently delayed at P7, while in c-Jun OE/OE mice, myelination was severely inhibited (Fig. 7D).

In c-Jun OE/+ mice, nerve area and the percentage of >1.5 μm diameter axons that were found within Schwann cell families or Remak bundles, both of which were normal in the adult, were also normal during development at all three time points (Fig. 7E,K). However, a number of other parameters were abnormal at P7, although they were normal at P1 and P21, revealing a transient delay in myelination. This includes the number of Schwann cell nuclei, which was elevated (Fig. 7F), the percentage of segregated (1:1), myelin-competent (>1.5μm diameter) axons that were myelinated, which was reduced, the total number of myelinated axons, which was reduced (Fig. 7H), and the number of segregated (1:1) myelin-competent (>1.5 μm diameter) axons that were not myelinated,

which was elevated (Fig. 7I). In adult nerves of these mice, the myelin sheaths are slightly thinner than in WT, and this difference was already present at P7 and P21 (Fig. 7J).

In the developing c-Jun OE/OE nerves, nerve area was not significantly different from that seen in WT or c-Jun OE/+ mice (Fig. 7E). The large nerve area in P60 nerves of these mice therefore emerges in adulthood. At P7 and P21 these nerves contained about twice the number of Schwann cell nuclei seen in WT nerves, a smaller difference than that seen in the adult (Fig. 7F). This suggests ongoing, low-level Schwann cell proliferation in adult mutant nerves, supported by Ki67 labelling of Sox10 positive Schwann cells, although the differences between WT and c-Jun OE/OE nerves in Cyclin D1 levels and did not reach significance (Fig. 7L,M). In other respects, the differences between developing WT and mutant nerves at P7 and P21 already matched those seen in adult P60 nerves. This includes a reduced number of myelinated axons, an increased number of segregated myelin competent axons that remained unmyelinated, thinner myelin sheaths, and an increased number of >1.5 µm diameter axons that were seen within Schwann cell families or Remak bundles (Fig. 6G-K).

These experiments show that c-Jun negatively regulates developmental myelination in a dose-dependent manner. In the c-Jun OE/+ mouse about six fold overexpression of c-Jun results in a transient delay at P7, while the nerve has recovered at P21. On the other hand, in the developing nerves of c-Jun OE/OE mice where c-Jun levels are about 50% higher than in c-Jun OE/+ nerves, myelination is permanently inhibited and seen in only 30-40% of >1.5µm myelin competent axons, a figure comparable to that seen in the adult.

Re-myelination after nerve injury in c-Jun OE/+ mice

c-Jun is a key amplifier of the repair Schwann cell phenotype, which is generated in the distal stump of injured nerves. Therefore, elevation of c-Jun is a candidate approach for improving nerve repair under conditions where it falters, such as in older animals or due to long term Schwann cell denervation (Wagstaff et al., 2017). The observation that in c-Jun OE/+ mice, adult nerves with about six fold elevation of c-Jun achieve a relatively normal degree of nerve architecture and myelination during development, albeit with a delay, is encouraging for this approach, since it demonstrates that significant c-Jun elevation and myelination are compatible. However, after injury, re-myelination is slower and more easily disrupted than developmental myelination. The two processes are also partly controlled by distinct signals. We therefore tested the capacity of c-Jun OE/+ nerves to re-myelinate after nerve injury.

After sciatic nerve crush injury, c-Jun levels distal to the crush were elevated in WT mice and this elevation was enhanced in c-Jun OE/+ mice as expected (Fig. 8A). At one, seven and 14 days after injury, c-Jun levels in OE/+ nerves were two to three fold higher than those in crushed WT control nerves. This amounted to about 12 (at one day after crush) to about 30 (at

seven and 14 days after crush) fold elevation of c-Jun in crushed c-Jun OE/+ nerves compared to the levels found in uninjured control nerves. This was accompanied by somewhat lower Krox20 levels (Fig. 8B). At 21 days after crush, c-Jun levels in WT nerves had declined although they still remained significantly above those in uninjured nerves (data not shown).

When examined four days after nerve cut, nerves of c-Jun OE/+ mice showed accelerated collapse/breakdown of myelin sheaths, and faster clearance of the myelin protein MBP, in agreement with previous evidence that c-Jun promotes myelin clearance and myelin autophagy (Arthur-Farraj et al 2012; Gomez-Sanchez et al. 2015) (Fig. 8C,D).

Examination of crushed c-Jun OE/+ nerves by electron microscopy showed a significant delay in re-myelination at 2 weeks after nerve crush (Fig. 8E). At this time point, about 35% of myelin-competent (>1,5µm) axons were myelinated in OE/+ nerves, while over 95% were myelinated in WT nerves (Fig. 8F). At two weeks after crush, the number of myelinated axons was also reduced in OE/+ nerves (Fig. 8G) and the number of segregated, myelin-competent axons without myelin was elevated (Fig. 8H). Significant recovery was seen four weeks after crush when about 75% of myelin-competent axons were myelinated in OE/+ nerves compared to 98% in WT nerves and by 10 weeks, essentially all myelin-competent axons were myelinated in both genotypes, a situation similar to that in uninjured nerves of these mice (Fig. 8E-H). Myelin sheaths in adult c-Jun OE/+ mice are thinner than in WT (previous section), and this difference was also seen in re-myelinated nerves (Fig. 8I). Tumours were not seen, and regenerating WT and c-Jun OE/+ nerves did not differ in size (Fig. 8J) or other aspects of general nerve architecture (Fig. 8E).

Importantly, the c-Jun OE/+ mice achieved full functional recovery after nerve crush. In the toe pinch test, which is primarily a sensory test, time to full recovery was comparable in WT and c-Jun OE/+ mice, while time to initial response (group average) was about 2 days longer in the mutants (Fig. 9A,B). In the toe spread reflex, primarily a test of motor recovery, c-Jun OE/+ mice showed a transient delay in recovery on days 14 and 15 only (Fig. 9C), possibly caused by delay in myelination at this time point (Fig. 8F,G). In the sciatic functional index (SFI) a sensory-motor test, c-Jun OE/+ mice showed a non-significant trend towards a transient delay during the second and third week after injury (Fig. 9D,E).

Discussion

We have generated c-Jun OE/+ and c-Jun OE/OE mice with enforced expression of c-Jun in Schwann cell nuclei to study the effects of a graded increase in c-Jun expression on Schwann cell development and on re-myelination after injury. This has shown, first, that during development and in adult nerves, Schwann cells are remarkably tolerant of elevated

c-Jun levels. Although developing and adult nerves of c-Jun OE/+ mice show about six fold increase in c-Jun relative to WT nerves at the same age, myelination is only transiently affected at P7. By P21, myelination appears normal, and in the adult, Schwann cells and nerve architecture is similar to that in WT nerves, with the exception of modestly reduced myelin thickness**,** which is unlikely to have significant consequences for sensory-motor control. Second, although re-myelination after injury, which generally is more easily perturbed than in development, is delayed in c-Jun OE/+ mice, re-myelination shows strong recovery at four weeks, and 10 weeks after injury essentially all myelin competent axons are myelinated. As in uninjured nerves, the myelin sheaths of regenerated OE/+ nerves remain thinner than those in regenerated WT nerves. The sensory and motor tests used here show only a slight delay followed by complete functional recovery in c-Jun OE/+ mice. Therefore, the c-Jun elevation in c-Jun OE/+ mice is compatible with essentially normal restoration of myelin and nerve function to that found before injury. This is important, because we find that the c-Jun elevation in c-Jun OE/+ mice is sufficient to accelerate regeneration under conditions where it is compromised by ageing or long-term denervation (Wagstaff et al, 2017; LJ Wagstaff, J Gomez-Sanchez, R Mirsky and KR Jessen unpublished). Third, the higher over-expression achieved in c-Jun OE/OE mice confirms the potential of c-Jun to negatively regulate myelination, as previously seen in vitro. Myelination is strongly impaired during development, and this persists in adult nerves, which show hypomyelinating pathology, enlarged connective tissue and immature onion bulbs. Fourth, even in nerves of aged c-Jun OE/OE mice, there is no evidence of tumour formation, and these nerves show strong activation of the tumour suppressor $P19^{ARF}$. The absence of tumorigenic effect of enforced c-Jun expression in Schwann cells is in agreement with the fact that mechanical nerve damage is not associated with tumour formation, although injured WT nerves contain proliferating cells with high c-Jun levels.

c-Jun is involved directly or indirectly in the control of about 180 of the approximately 4000 genes that change significantly after nerve injury. This allows c-Jun to take part in the regulation of a spectrum of properties of denervated repair Schwann cells, including morphology, autophagy-mediated myelin breakdown, and the expression of trophic factors linked to regeneration, including GDNF, artemin, BDNF, NGF and LIF (Arthur-Farraj et al., 2012; Fontana et al., 2012; Jessen et al 2015a; Gomez-Sanchez, 2015, Jessen and Mirsky, 2016). Of these GDNF, artemin and LIF have been shown to be direct targets of c-Jun. Additional evidence for direct regulation of injury-induced genes by c-Jun comes from a study of enhancer activation in Schwann cells. This showed c-Jun binding sites associated with injury-activated enhancers of genes elevated after nerve injury, including Shh, Olig1 and Runx2 (Hung et al., 2015).

The gene targets and function of AP-1 transcription factors, a family to which c-Jun belongs, are regulated by dimerization partners and ancillary proteins (Chinenov and Kerrpola 2001; Eferl and Wagner, 2003). Little is known about these components in Schwann cells.

The RNA sequencing analysis showed that in uninjured nerves of c-Jun OE/+ mice, 95 genes were expressed at levels that differed ≥2 fold from those in WT nerves. Sixty seven of these genes were up-regulated in response to increased c-Jun levels including *Shh* . In c-Jun OE/OE nerves, 1964 genes were changed ≥2 fold, and 909 of these were up-regulated, among them *GDNF, Shh, Olig1, Id2, Sox2 and Runx2.* The myelin genes *Mpz*, *Mbp* and *Pmp22* were all strongly down-regulated in c-Jun OE/OE nerves. Examining injured nerves, we previously, identified 172 genes that were expressed at different levels in seven day cut nerves of mice in which c-Jun was genetically inactivated compared to inured WT nerves. Of these 172 genes, 106 genes were up-regulated by higher c-Jun levels, namely expressed more highly in cut WT nerves than in cut c-Jun knockout nerves. A comparison of the 15 genes most up-regulated by c-Jun in uninjured c-Jun OE/+ and OE/OE nerves in the present work, with the 15 genes that are most up-regulated by c-Jun in seven day cut nerves reveals only two common genes, *Shh* and *GDNF*. This limited similarity indicates that the group of genes directly or indirectly regulated by c-Jun in Schwann cells that have adopted the repair phenotype after injury is significantly different from the set of genes, which responds to c-Jun in cells that ensheath axons, many of which retain myelin differentiation.

We find that the substantial c-Jun elevation in c-Jun OE/OE mice is sufficient to cause severe hypo-myelination**.** This is undoubtedly related to the ability of c-Jun to suppress myelin genes**.** Although the causal relationship between the increased c-Jun levels seen in human CMT1A, and demyelination has not been analysed (Hutton et al., 2011), it seems clear that sustained dys-regulation of c-Jun resulting in high expression in uninjured nerves is a potential hazard. c-Jun is therefore a candidate for a factor that could cause or promote pathological demyelination.

c-Jun OE/OE nerves and nerves affected by demyelinating neuropathies, in particular CMT1A, show many similarities, most obviously hypo-myelination. In c-Jun OE /OE mice, this involves substantially thinner myelin sheaths and about a 40% reduction in myelination among axons that have segregated and are myelin-competent. Axonal sorting is also adversely affected in younger (P60) c-Jun OE/OE mice, since in these mice, the percentage of unsorted >1.5 μm axons that remain in Remak bundles is 28%, compared to <1% in WT. In common with human CMT1A nerves, and nerves of the C22 and My41 mouse models of CMT1A, c-Jun OE/OE nerves also contain increased Schwann cell numbers (Robertson et al., 2002; Lupski and Chance 2005). However, neither mouse models of CMT1A nor the c-

595 Jun OE/OE mice show significant numbers of Schwann cells that are without axonal contact.
596 Increase in endoneurial connective tissue, which is substantial in c-Jun OE/OE mice, is also
597 a feature of human CMT1A nerves and of the CMT1A rat (Palumbo et al., 2002; Lupski and
598 Chance 2005; Fledrich et al., 2012). Abnormalities of Remak fibres, including the formation
599 of membranous structures that do not contact axons, which are seen in c-Jun OE/OE mice,
600 are also described in the My41, C22 and C3 mouse models of CMT1A (Robertson et al.,
601 2002; Verhamme et al., 2011). Lastly onion bulbs, which are prominent in human CMT1A
602 nerves and seen in rodent CMT1A models (Lupski and Chance 2005; Fledrich et al., 2012) ,
603 are also present in nerves of aged c-Jun OE/OE mice.

604 The histological changes outlined here for c-Jun OE/OE and CMT1A nerves, are generally
605 not specific to these conditions, but are also observed to a varying degree in a number of
606 other non-tumour-associated human nerve pathologies, mutant mouse nerves or in injured
607 nerves. (Low 1977; Haney et al., 1999; Chen et al., 2003; Ling et al. 2005; Kagitani-
608 Shimono 2008; Ishii et al., 2016). The relative paucity of disease-specific structural changes
609 in pathological nerves, and the sloppy relationship between molecular and histological
610 phenotype, makes it hard to interpret a particular histology in terms of a causal sequence.

611 Although the availability of binding partners or other ancillary proteins are important
612 regulators of c-Jun function, the levels of c-Jun protein are likely to be a key factor in
613 determining whether c-Jun has beneficial or adverse effects on nerve biology. Previous work
614 shows that already at low or moderate levels, which are compatible with myelination, c-Jun
615 appears to promote neuron-supportive signalling from Schwann cells to neurons, including
616 the activation of trophic factors, such as GDNF, while higher levels are required to suppress
617 myelin genes. Thus, in the C3 mouse model of CMT1A, c-Jun is elevated, but this is not high
618 enough to disrupt myelin, although it enhances axonal survival and sensory motor
619 performance (Hantke et al., 2014). Similarly, in CMT1X mice, c-Jun is elevated and
620 increases GDNF expression, but does not disrupt myelination (Klein et al., 2014).

621 In sum, the present results show that although moderate c-Jun increase is well tolerated
622 during Schwann cell development and re-myelination after injury, strong elevation of c-Jun in
623 uninjured nerves suffices to induce significant hypo-myelination pathology, implicating c-Jun
624 in demyelinating neuropathies. On the other hand, we do not find a link between c-Jun
625 elevation and tumorigenesis in line with the fact that tumours do not form after nerve injury,
626 although c-Jun is strikingly elevated as Schwann cells lose myelin differentiation and
627 proliferate. We also find that after crush injury of OE/+ nerves, myelination and nerve
628 function can be restored in the face of c-Jun levels that are high enough to promote axonal

regeneration in mice in which regeneration has been compromised by long term denervation or advanced age.

References

Ameyar-Zazoua M, Wisniewska MB, Bakiri L, Wagner EF, Yaniv M Weitzman JB (2005) AP-1 dimers regulate transcription of the p14/p19ARF tumor suppressor gene. Oncogene 24, 2298–2306.

Arthur-Farraj PJ, Latouche M, Wilton DK, Quintes S, Chabrol E, Banerjee A, Woodhoo A, Jenkins B, Rahman M, Turmaine M, Wicher GK, Mitter R, Greensmith L, Behrens A, Raivich G, Mirsky R, Jessen KR (2012) c-Jun reprograms Schwann cells of injured nerves to generate a repair cell essential for regeneration. Neuron 75:633-647.

Arthur-Farraj, PJ, Morgan CC, Adamowicz M, Gomez-Sanchez JA, Fazal,SV, Beucher A, Razzaghi B, Rhona Mirsky R, Jessen KR, Aitman TJ (2017) Changes in the Coding and Non-coding Transcriptome and DNA Methylome that Define the Schwann Cell Repair Phenotype after Nerve Injury. Cell Reports 20:2719-2734 .

Arthur-Farraj PJ, Wanek K, Hantke J, Davis CM, Jayakar A, Parkinson DB, Mirsky R, Jessen KR (2011) Mouse Schwann cells need both NRG1 and cyclic AMP to myelinate. Glia 59:720-733.

Brushart TM, Aspalter M, Griffin JW, Redett R, Hameed H, Zhou C, Wright M, Vyas A, Höke A (2013) Schwann cell phenotype is regulated by axon modality and central-peripheral location, and persists in vitro. Exp Neurol 247:272-281.

Chen S, Rio C, Ji RR, Dikkes P, Coggeshall RE, Woolf, CJ, Corfas G (2003) Disruption of ErbB receptor signaling in adult non-myelinating Schwann cells causes progressive sensory loss. Nature Neurosci 6: 1186 – 1193.

Chinenov Y, Kerppola TK (2001) Close encounters of many kinds: Fos-Jun interactions that mediate transcription regulatory specificity. Oncogene 20:2438-2452.

659 Collier H0, Warner BT, Sker R (1961) Multiple toe-pinch method for testing analgesic drugs.
660 Brit J Pharmacol17:28-40.

661 De Felipe C, Hunt SP (1994) The differential control of c-jun expression in regenerating
662 sensory neurons and their associated glial cells. J Neurosci 14:2911-2923.

663 Eferl R, Wagner EF (2003) AP-1: a double-edged sword in tumorigenesis. Nature Reviews
664 Cancer 3:859-868.

665 Eggers R, Tannemaat MR, Ehlert EM, Verhaagen J (2010) A spatio-temporal analysis of
666 motoneuron survival, axonal regeneration and neurotrophic factor expression after lumbar
667 ventral root avulsion and implantation. Exp Neurol 223:207-220.

668 Feltri ML, D'Antonio M, Previtali S, Fasolini M, Messing A, Wrabetz L (1999) P0-Cre
669 transgenic mice for inactivation of adhesion molecules in Schwann cells Ann N Y Acad Sci
670 883:116-123.

671 Fledrich R, Schlotter-Weigel B, Schnizer TJ, Wichert SP, Stassart RM, Meyer zuHörste G,
672 Klink A, Weiss BG, Haag U, Walter MC, Rautenstrauss B, Paulus W, Rossner MJ, Sereda
673 MW (2012) A rat model of Charcot-Marie-Tooth disease 1A recapitulates disease variability
674 and supplies biomarkers of axonal loss in patients. Brain 135:72-87.

675 Fontana X, Hristova M, Da Costa C, Patodia S, Thei L, Makwana M, Spencer-Dene B,
676 Latouche M, Mirsky R, Jessen KR, Klein R, Raivich G, Behrens A (2012) c-Jun in Schwann
677 cells promotes axonal regeneration and motoneuron survival via paracrine signaling. J Cell
678 Biol 198:127-141.

679 Gomez-Sanchez JA, Gomis-Coloma C, Morenilla-Palao C, Peiro G, Serra E, Serrano M,
680 Cabedo H (2013) Epigenetic induction of the Ink4a/Arf locus prevents Schwann cell
681 overproliferation during nerve regeneration and after tumorigenic challenge. Brain 136:2262-
682 2278.

683 Gomez-Sanchez JA, Carty L, Iruarrizaga-Lejarreta M, Palomo-Irigoyen M, Varela-Rey M,
684 Griffith M, Hantke J, Macias-Camara N, Azkargorta M, Aurrekoetxea I, De Juan VG,
685 Jefferies HB, Aspichueta P, Elortza F, Aransay AM, Martínez-Chantar ML, Baas F, Mato JM,
686 Mirsky R, Woodhoo A, Jessen KR (2015) Schwann cell autophagy, myelinophagy, initiates
687 myelin clearance from injured nerves. J Cell Biol 210:153-168.

688 Gomez-Sanchez JA, Lopez de Armentia M, Lujan R, Kessaris N, Richardson WD, Cabedo H
689 (2009) Sustained axon-glial signaling induces Schwann cell hyperproliferation, Remak
690 bundle myelination, and tumorigenesis. J Neurosci 29:11304-11315.

691 Haney CA, Sahenk Z,Li C, Lemmon VP, Roder J, Trapp BD (1999) Heterophilic Binding of
692 L1 on Unmyelinated Sensory Axons Mediates Schwann Cell Adhesion and Is Required for
693 Axonal Survival. J Cell Biol 146: 1173-1183.

694 Hantke J, Carty L, Wagstaff LJ, Turmaine M, Wilton DK, Quintes S, Koltzenburg M, Baas F,
695 Mirsky R, Jessen KR (2014) c-Jun activation in Schwann cells protects against loss of
696 sensory axons in inherited neuropathy. Brain 137:2922-2937.

697 Hung HA, Sun G, Keles S, Svaren J (2015) Dynamic regulation of Schwann cell enhancers
698 after peripheral nerve injury. J Biol Chem 290:6937-6950.

699 Hutton EJ, Carty L, Laurá M, Houlden H, Lunn MP, Brandner S, Mirsky R, Jessen K, Reilly
700 MM (2011) c-Jun expression in human neuropathies: a pilot study. J Peripher Nerv Syst
701 16:295-303.

702 Ishii A, Miki Furusho, Dupree JL, Bansal R (2016) Strength of ERK1/2 MAPK Activation
703 Determines Its Effect on Myelin and Axonal Integrity in the Adult CNS. J Neurosci 36:6471-
704 6487.

705 Jessen KR, Mirsky R (2008) Negative regulation of myelination: relevance for development,
706 injury, and demyelinating disease. Glia 56:1552-1565.

707 Jessen KR, Mirsky R, Arthur-Farraj P (2015a) The Role of Cell Plasticity in Tissue Repair:
708 Adaptive Cellular Reprogramming. Dev Cell. 34:613-620.

709 Jessen KR, Mirsky R, Lloyd AC (2015b) Schwann Cells: Development and Role in Nerve
710 Repair. Cold Spring Harb Perspect Biol doi: 10.1101/cshperspect.a020487.

711 Jessen, K. R. and Mirsky, R (2016) The repair Schwann cell and its function in regenerating
712 nerves. J Physiol 594: 3521–3531.

713 Kagitani-Shimono K, Mohri I, Yagi T, Taniike M, Suzuki K (2008) Peripheral neuropathy in
714 the twitcher mouse: accumulation of extracellular matrix in the endoneurium and aberrant
715 expression of ion channels. Acta Neuropathol 115:577-587.

716 Klein D, Groh J, Wettmarshausen J, Martini R (2014) Nonuniform molecular features of
717 myelinating Schwann cells in models for CMT1: distinct disease patterns are associated with
718 NCAM and c-Jun upregulation. Glia 62:736-750.

719 Ling BC, Wu J, Miller SJ, Monk KR, Shamekh R, Rizvi TA, Decourten-Myers G, Vogel KS,
720 DeClue JE, Ratner N (2005) Role for the epidermal growth factor receptor in
721 neurofibromatosis-related peripheral nerve tumorigenesis. Cancer Cell 7:65-75.

722 Low PA (1977) The evolution of “onion bulbs” in the hereditary hypertrophic neuropathy of
723 the Trembler mouse. Neuropathol and Appl Neurobiol 3:81-92

724 Lupski JR, Chance PF (2005) Hereditary motor and sensory neuropathies involving altered
725 dosage or mutation of PMP22: The CMT1A Duplication and and HNPP deletion. In:
726 Peripheral Neuropathy (PJ Dyck PJ and Thomas PK, ed), pp1659-1680. Philadelphia:
727 Elsevier Inc.

728 Ma CH, Omura T, Cobos EJ, Latrémolière A, Ghasemlou N, Brenner GJ, van Veen E,
729 Barrett L, Sawada T, Gao F, Coppola G, Gertler F, Costigan M, Geschwind D, Woolf CJ
730 (2011) Accelerating axonal growth promotes motor recovery after peripheral nerve injury in
731 mice. J Clin Invest 121:4332-4347.

732 Meier C, Parmantier E, Brennan A, Mirsky R, Jessen KR (1999) Developing Schwann cells
733 acquire the ability to survive without axons by establishing an autocrine circuit involving
734 insulin-like growth factor, neurotrophin-3, and platelet-derived growth factor-BB. J Neurosci
735 19:3847-3359.

736 Morgan L, Jessen KR, Mirsky R (1991) The effects of cAMP on differentiation of cultured
737 Schwann cells: progression from an early phenotype (04+) to a myelin phenotype (P0+,
738 GFAP-, N-CAM-, NGF-receptor-) depends on growth inhibition. J Cell Biol 112:457-467.

739 Olsson Y (1971) Mast cells in human peripheral nerve. Acta Neurol Scand 47:357-368.

740 Painter MW, Brosius Lutz A, Cheng YC, Latremoliere A, Duong K, Miller CM, Posada S,
741 Cobos EJ, Zhang AX, Wagers AJ, Havton LA, Barres B, Omura T, Woolf CJ (2014)
742 Diminished Schwann cell repair responses underlie age-associated impaired axonal
743 regeneration. Neuron 83:331-343.
744

745 Palumbo C, Massa R, Panico MB, Di Muzio A, Sinibaldi P, Bernardi G, Modesti A (2002)
746 Peripheral nerve extracellular matrix remodeling in Charcot-Marie-Tooth type I disease. Acta
747 Neuropathol 104:287-296.

748 Parkinson DB, Bhaskaran A, Arthur-Farraj P, Noon LA, Woodhoo A, Lloyd AC, Feltri ML,
749 Wrabetz L, Behrens A, Mirsky R, Jessen KR (2008) c-Jun is a negative regulator of
750 myelination. J Cell Biol 181:625-637.

751 Parkinson DB, Bhaskaran A, Droggiti A, Dickinson S, D'Antonio M, Mirsky R, Jessen KR
752 (2004) Krox-20 inhibits Jun-NH2-terminal kinase/c-Jun to control Schwann cell proliferation
753 and death. J Cell Biol 164:385-394.

754 Roberts SL, Dun X, Doddrell RDS, Mindos T, Drake LK, Onaitis MW, Florio F, Quattrini A,
755 Lloyd AC, D'Antonio M,Parkinson DB (2017) Sox2 expression in Schwann cells inhibits
756 myelination in vivo and induces influx of macrophages to the nerve. Development 144: 3114-
757 3125

758 Robertson AM, Perea J, McGuigan A, King RH, Muddle JR, Gabreëls-Festen AA, Thomas
759 PK, Huxley C (2002) Comparison of a new pmp22 transgenic mouse line with other mouse
760 models and human patients with CMT1A. J Anat 200:377-390.

761 Shaulian E (2010) AP-1 — The Jun proteins: Oncogenes or tumor suppressors in disguise?
762 Cellular Signalling. 22: 894–899.

763 Shy ME, Shi Y, Wrabetz L, Kamholz J, and Scherer SS (1996) Axon-Schwann Cell
764 Interactions Regulate the Expression of c-jun in Schwann Cells. J Neurosci Res 43:511-525.

765 Truett GE, Heeger P, Mynatt RL, Truett AA, Walker JA and Warman ML (2000) Preparation
766 of PCR-Quality mouse genomic DNA with hot sodium hydroxide and tris (HotSHOT).
767 BioTechniques 29:52-54.

768 Verhamme C, King RH, ten Asbroek AL, Muddle JR, Nourallah M, Wolterman R, Baas F,
769 van Schaik IN (2011) Myelin and axon pathology in a long-term study of PMP22-
770 overexpressing mice. J Neuropathol Exp Neurol 70:386-398.

771 Wagstaff, LJ, Gomez-Sanchez, JA, Mirsky, R, Jessen, KR (2017) The relationship between
772 Schwann cell c-Jun and regeneration failures due to ageing and long-term injury. Glia
773 65,S1:E532.

774 Yang FC, Ingram DA, Chen S, Hingtgen CM, Ratner N, Monk KR, Clegg T, White H, Mead
775 L, Wenning MJ, Williams DA, Kapur R, Atkinson SJ, Clapp DW (2003) Neurofibromin-
776 deficient Schwann cells secrete a potent migratory stimulus for Nf1+/- mast cells. J Clin Inv
777 112:1851-1861.

778

779

780

781

782

783

784

Figure legends

Figure 1. Graded over-expression of c-Jun Schwann cell nuclei of c-Jun OE/+ and c-Jun OE/OE mice.

(A) Genomic structure of the c-Jun floxed allele in the Rosa26 locus. Excision of the stop codon is effected by crossing Rosa26c-Junff/+ mice with P0cre expressing mice to generate c-Jun OE/+ and c-Jun OE/OE mice over-expressing c-Jun specifically in Schwann cells.

(B) PCR analysis showing the presence of c-Jun OE, Rosa26 WT and P0cre bands from DNA samples extracted from tails of WT, c-Jun OE/+ and c-Jun OE/OE mice.

(C) Representative immunofluorescence images from WT, OE/+ and OE/OE sciatic nerve cryosections showing Sox10 and c-Jun positive nuclei. Note graded increase in c-Jun in c-JunOE/+ and c-Jun OE/OE mice. Scale bar; 50μm.

(D) Western blot of sciatic nerve protein extracts from P60 WT, c-Jun OE/+ and c-Jun OE/OE mice showing increasing c-Jun levels. The graph quantifies c-Jun expression in WT (n=7), c-Jun OE/+ (n=6) and c-Jun OE/OE (n=6) mice. The quantifications are normalized to the levels in uninjured WT nerves, which are set as 1. Note that the difference in c-Jun expression between c-Jun OE/+ and c-Jun OE/OE nerves is also significant. One-way ANOVA with Tukey comparison; *$p<0.05$, ****$p<0.0001$.

(E) Representative immunofluorescence images from purified Schwann cell cultures from WT and c-Jun OE/+ mice. The cells were exposed to neuregulin (nrg) alone, or neuregulin plus cAMP analogue (dbcAMP), a combination that mimics axonal myelination signals. Note that neuregulin plus dbcAMP suppresses c-Jun in WT, but not in c-Jun OE/+, cells. Sox10 was used as a Schwann cell marker to show levels of c-Jun specifically in Schwann cells.

Figure 2. Gene expression in c-Jun OE/+ and c-Jun OE/OE mice.

(A) Heat map of the 400 most regulated genes in uninjured nerves of WT and c-Jun OE/OE mice.

(B) PCA map of gene regulation in WT and c-Jun OE/OE nerves

(C) Expression of 13 genes of interest in the sciatic nerve of OE/+ and OE/OE mice.

The table shows how c-Jun elevation affects the expression of a sub-set of repair cell markers, myelin proteins and transcription factors in the mouse lines indicated. Note that in OE/+ nerves, only *Shh* is regulated ≥2 fold. In OE/OE nerves, repair cell markers are up-

regulated, and myelin genes are down-regulated, although two important myelin regulators, *Krox20* and *Sox10* are not strongly affected. WT (n=3), OE/+ (n=4) and OE/OE (n=4).

Figure 3. The 15 most up- and down-regulated genes in the sciatic nerve of OE/+ and OE/OE mice.

(A and B) The 15 most strongly elevated genes (the upper panels) and the 15 most suppressed genes (the lower panels) in response to c-Jun elevation in the mouse lines indicated.

(C) The 15 most strongly regulated gene in OE/OE nerves compared to expression in OE/+ nerves.

(D) Representative immunofluorescence images from WT, c-Jun OE/+ and c-Jun OE/OE sciatic nerve cryosections showing Krox20 in Sox10 positive Schwann cell nuclei. Note similar Krox20 expression in WT and c-Jun OE/+ nerves, but much reduced levels in c-Jun OE/OE nerves. Scale bar: 50μm.

(E) Western blot of sciatic nerve protein extracts from P60 mice showing similar levels of Krox20 in WT and c-Jun OE/+ nerves, but lower levels in c-Jun OE/OE nerves. The graph quantifies Krox20 expression in WT (n=5), c-Jun OE/+ (n=4) and c-Jun OE/OE (n=5) mice. The quantifications are normalized to the levels in uninjured WT nerves, which are set as 1. One-way ANOVA with Tukey comparison; *p<0.05, **p<0.01.

(F) Western blot of sciatic nerve protein extracts from P60 mice. Note that Mpz expression is 15% lower than WT in c-Jun OE/+ nerves, but strongly suppressed in c-Jun OE/OE nerves. The graph quantifies Mpz expression in WT (n=5), c-Jun OE/+ (n=4) and c-Jun OE/OE (n=5) mice. The quantifications are normalized to the levels in uninjured WT nerves, which are set as 1. One-way ANOVA with Tukey comparison; ****p<0.0001.

Figure 4. Electron Microscopic structure of adult nerves in WT and OE/+ mice.

(A) Electron micrographs showing similar overall appearance of nerves from P60 WT and OE/+ mice. Scale bar: 5μm.

(B) The total area of P60 WT and OE/+ mouse nerves is not significantly different. Mann-Whitney U test; p=0.5317 (n=5).

(C) The number of Schwann cell nuclei per sciatic nerve profiles not significantly different between P60 WT and OE/+ nerves. Mann-Whitney U test; p=0.0952 (n=5).

(D) Counts of Ki67 positive/Sox10 positive nuclei indicate that the difference in Schwann cell proliferation between WT and c-Jun OE/+ mice is not significantly different. Mann-Whitney U test; p=0.2000 (n=3).

(E) The total number of axons larger than 1.5μm in diameter is similar in P60 WT and OE/+ nerves. Mann-Whitney U test; p=0.9444 (n=5).

(F) The percentage of axons in a 1: 1 relationship and greater than 1.5μm in diameter that are myelinated is similar in P60 WT and OE/+ nerves. Mann-Whitney U test; p>0.9999 (n=5).

(G) Per nerve profile, the number of myelinated axons is similar in P60 WT and OE/+ nerves. Mann-Whitney U test; p=0.8016 (n=5).

(H) Per nerve profile, the number of axons in a 1:1 relationship and greater than 1.5μm in diameter but not myelinated is not significantly different between P60 WT and OE/+nerves. Mann-Whitney U test; p>0.999 (n=5).

(I) Myelin thickness measured by g-ratios is thinner in P60 OE/+ nerves compared to WT. The whiskers extend from the 5^{th} to the 95^{th} percentiles. Mann-Whitney U test; p=0.0079 (n=5).

(J) The percentage of axons greater than 1.5μm in diameter that remain unmyelinated and within Remak bundles is very low and similar in P60 WT and OE/+ nerves. Mann-Whitney U test; p=0.1508 (n=5).

(K) Electron micrographs show that the overall structure of adult P300 nerves in WT and OE/+mice is similar. Scale bar: 5μm.

(L) The area of transverse profiles of P300 WT (n=4) and OE/+ (n=5) nerves is not statistically different. Mann-Whitney U test; p=0.2857.

(M) The number of Schwann cell nuclei per sciatic nerve profile is somewhat higher in P300 OE/+ (n=5) nerves compared to WT (n=4). Mann-Whitney U test; p=0.0317.

(N) The total number of axons larger than 1.5μm in diameter is similar in P300 WT (n=4) and c-Jun OE/+ (n=5) nerves. Mann-Whitney U test; p=0.1905.

(O)The percentage of axons in a 1: 1 relationship and greater than 1.5 μm in diameter that are myelinated is similar in P300 WT (n=4) and OE/+ (n=5) nerves. Mann-Whitney U test; p=0.4444.

(P) The numbers of myelinated axons per nerve profile is similar in P300 WT (n=4) and OE/+ (n=5) nerves. Mann-Whitney U test; p=0.1905.

(Q) Per nerve profile, the number of axons that are greater than 1.5μm in diameter and in a 1:1 relationship but not myelinated is not significantly different between P300 WT (n=4) and OE/+ (n=5) nerves. Mann-Whitney U test; p=0.4444.

(R) Measured by g-ratios, myelin is thinner in P300 OE/+ (n=5) nerves than in WT (n=4). The whiskers extend from the 5^{th} to the 95^{th} percentiles. Mann-Whitney U test; p=0.0079.

(S) The percentage of unmyelinated axons greater than 1.5μm in diameter that remain in Remak bundles is similar in P300 WT (n=4) and OE/+ (n=5) nerves. Mann-Whitney U test; p>0.9999.

Figure 5. High c-Jun levels in c-Jun OE/OE nerves result in hypo-myelination.

(A) Electron micrographs showing lack of myelin and increased connective tissue spaces in P60 c-Jun OE/OE nerves compared to WT.

(B) The total number of axons larger than 1.5μm in diameter is not significantly different in P60 WT (n=5) and c-Jun OE/OE (n=3) nerves. Mann-Whitney U test; p=0.0714.

(C) The percentage of axons in a 1: 1 relationship and greater than 1.5μm in diameter that are myelinated is lower in c-Jun OE/OE mice than in WT (n=5) and OE/OE (n=3) nerves. Mann-Whitney U test; p=0.0179.

(D) The number of myelinated axons per nerve profile is substantially reduced in c-Jun OE/OE (n=3) nerves compared to WT (n=5). Mann-Whitney U test; p=0.0357.

(E) Per nerve profile, the number of axons in a 1:1 relationship and greater than 1.5μm in diameter but not myelinated is much higher in OE/OE (n=3) nerves than in WT (n=5). Mann-Whitney U test; p=0.0179.

(F) Myelin, measured as g-ratios, is thinner in OE/OE (n=3) mice compared to WT (n=5). The whiskers extend from the 5^{th} to the 95^{th} percentiles. Mann-Whitney U test; p=0.0357.

(G) The percentage of unmyelinated axons greater than 1.5μm in diameter that remain in Remak bundles is higher in OE/OE (n=3) nerves than in WT (n=5) nerves. Mann-Whitney U test; p=0.0357.

(H) Nerves in c-Jun OE/OE mice (n=3) contain more mast cells that nerves in WT mice (n=5). Mann-Whitney U test; p=0.0179.

(I) OE/OE (n=3) nerves show more Schwann cell nuclei per nerve profile than WT (n=5) nerves. Mann-Whitney U test; p=0.0357.

(J) Western blot of sciatic nerve protein extracts from P60 mice. Note that levels of Cyclin D1 (a marker of cell proliferation) are significantly higher in OE/OE nerves than in WT or OE/+ or nerves. The results are quantified in the graph; WT (n=5), OE/+ (n=4) and OE/OE (n=5). The quantifications are normalized to the levels in uninjured WT nerves, which are set as 1. One-way ANOVA with Tukey comparison; *p<0.05, **p<0.01.

(K) Counts of Ki67 positive/Sox10 positive nuclei indicate a higher rate of Schwann cell proliferation in c-Jun OE/OE mice (n=5) compared to WT (n=3). Mann-Whitney U test; p=0.0179.

(L) The area of transverse profiles of OE/OE (n=3) nerves is larger than of WT nerves. Mann-Whitney U test; p=0.0357 (n=5).

(M) Tracing of cell profiles and extracellular space (ECM) in transverse nerve sections, followed by area measurements, shows a relative increase in extracellular space in OE/OE (n=3) nerves compared to WT (n=5). Mann-Whitney U test; p=0.0357.

(N) Western blot of sciatic nerve protein extracts from P60 mice. Note increased expression of the tumor suppressor p19ARF. The results are quantified in the graph. The quantifications are normalized to the levels in uninjured WT nerves, which are set as 1. One-way ANOVA with Tukey comparison; *p<0.05 (n=3).

Figure 6. Nerves of aged c-Jun OE/OE mice

(A) The nerves of P300 c-Jun OE/OE mice and WT mice contain comparable numbers of axons. Mann-Whitney U test; p=0.1143 (n=4).

(B) In P300 c-Jun OE/OE mice the percentage of axons in a 1: 1 relationship and greater than 1.5μm in diameter that are myelinated is lower than in WT mice. Mann-Whitney U test; p=0.0286 (n=4).

(C) In P300 c-Jun OE/OE mice, the number of myelinated axons per nerve profile is reduced compared to WT. Mann-Whitney U test; p=0.0286 (n=4).

(D) Per nerve profile, P300 c-Jun OE/OE mice have a much larger number of unmyelinated axons that are greater than 1.5μm in diameter and in a 1:1 relationship and, compared to WT mice Mann-Whitney U test; p=0.0286 (n=4).

(E) The percentage of unmyelinated axons greater than 1.5μm in diameter that are found within Remak bundles is higher in OE/OE nerves than in WT nerves. Mann-Whitney U test; p=0.0286 (n=4).

(F) Electron micrographs from nerves of P300 c-Jun OE/OE mice, showing examples of onion bulbs. The central axon, which is sometimes myelinated (upper panels), is surrounded by relatively few layers of flattened Schwann cells, suggesting an early stage of bulb formation. Scale bar = 1 μm.

(G) The number of onion bulbs in P300 OE/OE nerves is much higher than in WT nerves. Mann-Whitney U test; p=0.0286 (n=4).

(H) P300 OE/OE nerves contain a higher number of mast cells than WT nerves. Mann-Whitney U test; p=0.0286 (n=4).

(I) Nerves in P300 c-Jun OE/OE mice show more Schwann cell nuclei per nerve profile than nerves in WT mice. Mann-Whitney U test; p=0.0286 (n=4).

(J) The rate of Schwann cell proliferation is not significantly higher in P300 OE/OE nerves than in WT nerves, judged by counts of Ki67 positive/Sox10 positive nuclei. Mann-Whitney U test; p=0.1000 (n=3).

Figure 7. Developmental over-expression of c-Jun delays myelination in c-Jun OE/+ mice, but inhibits myelination in c-Jun OE/OE mice.

(A) Western blot of nerve extracts from P1 and P7 sciatic nerves. The results are quantified in the graphs**.** Data from P1 nerves are normalized to levels in P1 WT nerve, which are set as 1, while data from P7 nerves are normalized to levels in P7 WT nerve, which are set as 1. Note that by P7, c-Jun is elevated in both OE/+ and OE/OE nerves, while Mpz is reduced in OE/OE nerves only. P1 WT (n=3), OE/+(n=3); P7 WT (n=4); OE/+ (n=4), OE/OE (n=3). Statistical analysis for P1 is Student`s T-test; p=0.0608 for c-Jun, p=0.0174 for Mpz. Statistical analysis for P7 is One-way ANOVA with Tukey comparison; *p< 0.05, **p<0.01, ****p<0.0001.

(B) Western blot of nerve extracts from P7 WT, OE/+ and OE/OE nerves. The results are quantified in the graph. Krox20 levels are similar in all genotypes. One-way ANOVA with Tukey comparison; p=0.2053 (n=3).

(C) The percentage of Krox20/Sox10 positive Schwann cells in sections from WT (n=8), OE/+ (n=6) and OE/OE (n=3) sciatic nerves at P7. Note a graded decrease in Krox20 positive cells as levels of c-Jun increase. One-way ANOVA with Tukey comparison; *p<0.05, ***p<0.001.

(D) Representative electron micrographs from P1, P7 and P21 nerves of WT, c-Jun OE/+ and c-Jun OE/OE mice. Note hypomyelination in OE/OE nerve at P7 and P21, and transient hypomyelination in OE/+ nerves at P7. Scale bar= 5μm.

(E) The nerve areas are similar in all three genotypes at all developmental stages. One-way ANOVA with Tukey comparison; P1 WT (n=5), OE/+ (n=4) and OE/OE (n=5), p=0.1978; P7 WT (n=5), OE/+ (n=5) and OE/OE (n=3), p=0.2261 and P21 WT (n=5), OE/+ (n=4) and OE/OE (n=4), p=0.084.

(F). The number of Schwann cell nuclei per sciatic nerve profile at P1, P7 and P21 in nerves of WT, c-Jun OE/+ and c-Jun OE/OE mice. Note the transient difference between WT and OE/+ nerves at p7, while OE/OE nerves have more Schwann cells at p7 and p21. P1 WT (n=5), OE/+ (n=4) and OE/OE (n=5); P7 WT (n=5), OE/+ (n=5) and OE/OE (n=3); and P21 WT (n=5), OE/+ (n=4) and OE/OE (n=4). One-way ANOVA with Tukey comparison. **p< 0.01, ***p<0.001 and ****p<0.0001.

(G) The percentage of axons in a 1: 1 relationship and greater than 1.5μm in diameter that are myelinated at P1, P7 and P21 in nerves of WT, c-Jun OE/+ and c-Jun OE/OE mice. Note reduced myelination in OE/OE mice at P7 and 21, and transient reduction in OE/+ mice at P7. P1 WT (n=5), OE/+ (n=4) and OE/OE (n=5); P7 WT (n=5), OE/+ (n=5) and OE/OE (n=3); and P21 WT (n=5), OE/+ (n=4) and OE/OE (n=4). One-way ANOVA with Tukey comparison; **p<0.01 and ***p<0.001

(H) The number of myelinated axons per nerve profile at P1, P7 and P21 in nerves of WT, c-Jun OE/+ and c-Jun OE/OE mice. Note the substantial reduction in myelinated axons in OE/OE nerves at P7 and P21, and transient decrease in OE/+ mice at P7. P1 WT (n=5), OE/+ (n=4) and OE/OE (n=5); P7 WT (n=5), OE/+ (n=5) and OE/OE (n=3); and P21 WT (n=5), OE/+ (n=4) and OE/OE (n=4). One-way ANOVA with Tukey comparison; *p<0.05, **p<0.01, ***p<0.001 and ****p<0.0001.

(I) The number of axons in a 1:1 relationship and greater than 1.5μm in diameter that remain unmyelinated at P1, P7 and P21 in nerves of WT, c-Jun OE/+ and c-Jun OE/OE mice. Note the increase in unmyelinated axons in OE/OE nerves at P7 and P21, but at p7 only in OE/+ mice. P1 WT (n=5), OE/+ (n=4) and OE/OE (n=5); P7 WT (n=5), OE/+ (n=5) and OE/OE (n=3); and P21 WT (n=5), OE/+ (n=4) and OE/OE (n=4). One-way ANOVA with Tukey comparison; **p<0.01, ***p<0.001 and ****p<0.0001

(J) In both OE/+ and OE/OE nerves, the reduction in myelin thickness, measured as g-ratios, which is seen in the adults is already present at P7 and p21. P7 WT (n=5), OE/+ (n=5) and OE/OE (n=3); and P21 WT (n=5), OE/+ (n=4) and OE/OE (n=4). The whiskers

extend from the 5th to the 95th percentiles. One-way ANOVA with Tukey comparison, *p<0.05, **p<0.01, and ***=p<0.001.

(K) The percentage of unmyelinated axons that are greater than 1.5μm in diameter in Schwann cell families or Remak bundles at P1, P7 and P21 in nerves of WT, c-Jun OE/+ and c-Jun OE/OE mice. Abnormally high numbers are seen in OE/OE nerves only. P1 WT (n=5), OE/+ (n=4) and OE/OE (n=5); P7 WT (n=5), OE/+ (n=5) and OE/OE (n=3); and P21 WT (n=5), OE/+ (n=4) and OE/OE (n=4). One-way ANOVA with Tukey comparison, *p<0.05, **p<0.01, and ***p<0.001.

(L) Western blot of nerve extracts from P7 WT (n=3), OE/+ (n=3) and OE/OE (n=3) sciatic nerves showing Cyclin D1, an indicator of cell proliferation. Quantification of the data is normalized to levels in P7 WT nerve, which are set as 1. Cyclin D1 levels are similar in all mouse lines. One-way ANOVA with Tukey comparison; p=0.3871.

(M) Counts of Ki67 positive/Sox10 positive nuclei in P7 in WT (n=6), OE/+ (n=6) and OE/OE (n=3) nerves. OE/OE nerves show increased Schwann cell proliferation. One-way ANOVA with Tukey comparisons, *p=0,0121. In Figs. E-K, p values are calculated relative to WT at the same age.

Figure 8. Re-myelination of OE/+ nerves is delayed

(A) Western blot of c-Jun in nerve extracts from the distal stump of adult WT (n=4) and OE/+ (n=4) nerves 1 day, 7 days and 2 weeks after crush. The graph shows quantification of the results, normalized to levels in uninjured WT nerves, which are set as 1. Note significant elevation of c-Jun at all time points. Mann-Whitney U test: 1 day p=0.0006 (n=4); 7 days p=0.0002 (n=4); and 2 weeks p=0.0022(n=4).

(B) Western blot of nerve extracts from the distal stump of adult WT and OE/+ nerves 2 weeks after crush. The results are quantified in the graph, normalized to levels in 2 week crushed WT nerve, which are set as 1. Krox20 levels are reduced in OE/+ nerves. Mann-Whitney U test, p=0.0286, (n=4).

(C) Representative electron micrographs from the distal stump 4 days after sciatic nerve cut in WT and c-Jun OE/+ mice, illustrating collapsed myelin sheaths. The graph shows that fewer intact myelin sheaths per nerve profile remain in OE/+ nerves than in WT; Mann-Whitney U test; p=0.0286 (n=4).

(D) Transected c-Jun OE/+ nerves clear myelin protein faster than WT nerves. The graph shows the reduction in MBP 4 days after transection expressed as a percentage of MBP in

uninjured nerve. WT and c-Jun OE/+ nerves have cleared close to 40% and 60% of their MBP content, respectively. The data are obtained from quantitation of Western blots. WT (n=4) and OE/+ (n=8). Mann-Whitney U test; p=0.0070.

(E) Representative electron micrographs from the distal stump of WT and OE/+ nerves 2, 4 and 10 weeks after crush. In OE/+ nerves, the number of myelinated axons, which is reduced at 2 and 4 weeks, has recovered at 10 weeks. Scale bar: 5μm.

(F) The percentage of axons greater than 1.5μm in diameter and in a 1:1 ratio that are myelinated in the distal stump of WT and c-Jun OE/+ mice 2, 4 and 10 weeks after nerve crush. Note that myelination in OE/+ nerves, which is reduced at 2 weeks, has recovered substantially by 4 weeks and is normal at 10 weeks. Mann-Whitney U test: 2 weeks p=0.0286, n=4; 4 weeks P=0.0079, n=5; and 10 weeks p=0.0571 (n=4).

(G) The number of myelinated axons per nerve profile of the distal stump of WT and c-Jun OE/+ mice 2, 4 and 10 weeks after nerve crush. In c-Jun OE/+ mice, few myelinated axons are present at 2 weeks, but normal numbers are seen at 10 weeks. Mann-Whitney U test: 2 weeks p=0.0286 (n=4); 4 weeks p=0.0079 (n=5); and 10 weeks p=0.0571 (n=4).

(H) The number of unmyelinated axons greater than 1.5μm in diameter and in a 1:1 relationship that have not myelinated in the distal stump of WT and OE/+ nerves 2, 4 and 10 weeks after crush. Two and 4 week crushed OE/+ nerves contain elevated numbers of umyelinated axons, but their number has fallen to normal levels at 10 weeks. Mann-Whitney U test: 2 weeks p=0.0286 (n=4); 4 weeks P=0.0079 (n=5); and 10 weeks p=0.1143 (n=4).

(I) Myelin thickness, measured as g-ratios, is reduced in the distal stump of OE/+ nerves at all time points after crush. The whiskers extend from the 5^{th} to the 95^{th} percentiles. Mann-Whitney U test: 2 weeks p=0.0286 (n=4); 4 weeks p=0.0079 (n=5); and 10 weeks p=0.0286 (n=4).

(J) The area of transverse sections through the distal stump 2,4 and 10 weeks after crush is similar in WT and OE/+ nerves. Mann-Whitney U test: 2 weeks p=0.6571 (n=4); 4 weeks p=0.3095 (n=5); and 10 weeks p=0.9004 (n=4).

In Figs. A and F-J, p values are calculated relative to WT at same time after injury.

Figure 9. Functional recovery is slightly delayed in c-Jun OE/+ mice.

(A) Toe pinch assay, showing the percentage of mice that show a response to a pinch of toes 3, 4 and 5 at different times after sciatic nerve crush in WT and c-Jun OE/+ mice. In c-Jun OE/+ mice, all toes show a trend towards a delayed response.

(B) The average time in days after crush at which the first toe pinch response is seen in toe 3, toe 4 and toe 5. WT (n=10) and OE/+ (n=9). Mann-Whitney U test; p values are calculated relative to WT for each toe. Toe 3 p=0.0056, Toe 4 p= 0.0043, Toe 5 p= 0.0404.

(C) The toe spread reflex in WT (n=10) and OE/+ (n=9) mice following sciatic nerve crush. The reflex response is delayed at day12, 14 and 15 in c-Jun OE/+ mice. Two-way ANOVA with Bonferroni comparison, p=0.0171.

(D) Representative digital footprints from WT and c-Jun OE/+ mice taken at 0, 7, 18, 21, 28 and 70 days after sciatic nerve crush, used in sciatic functional index (SFI) analysis.

(E) SFI results from WT (n=11) and c-Jun OE/+ (n=8) mice at different times after sciatic nerve crush. There is no significant difference between WT and c-Jun OE/+ mice. Two-way ANOVA with Bonferroni comparison, p=0.5545.

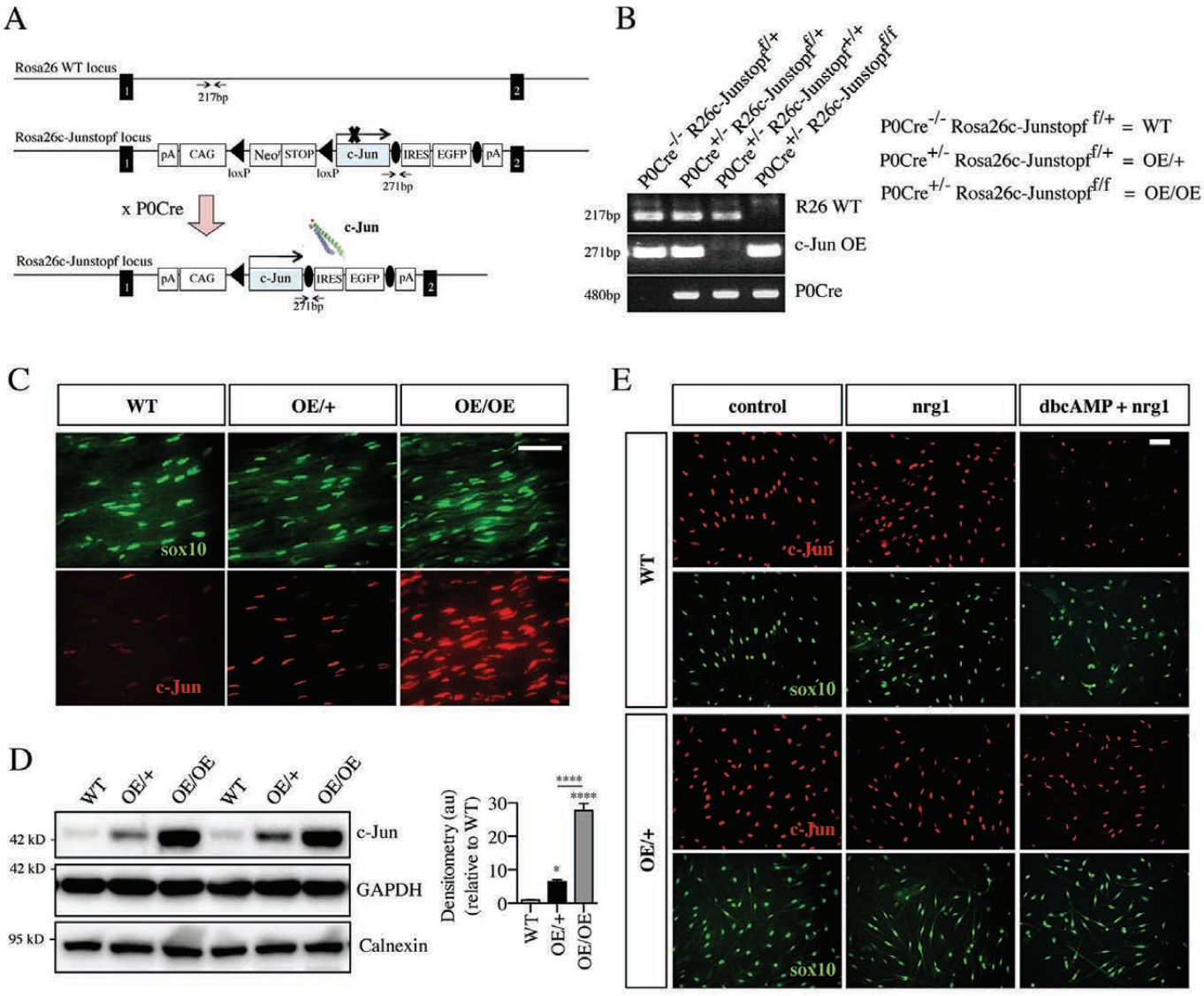

A

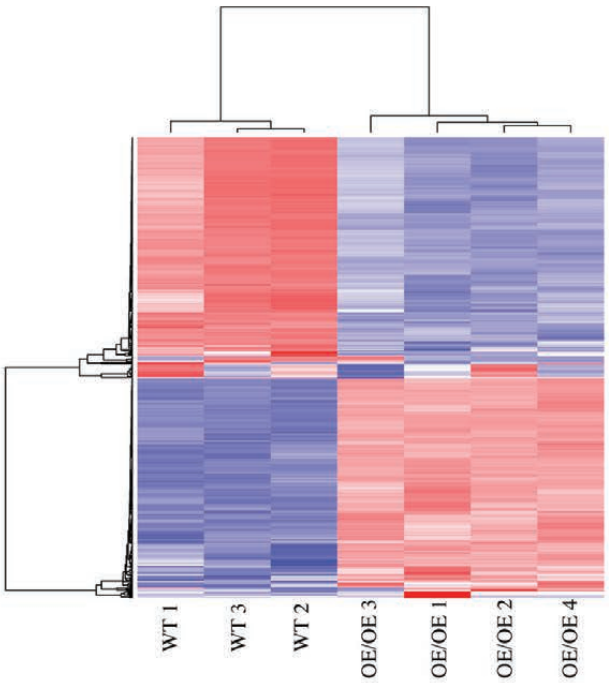

B

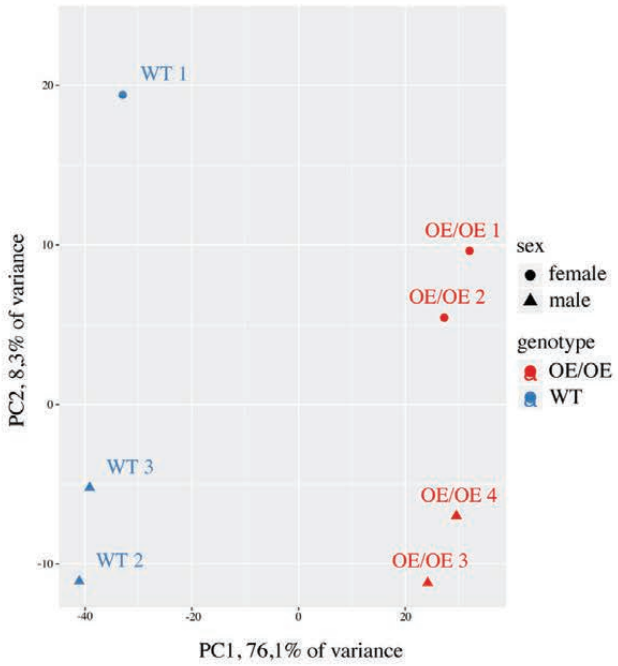

C

	Gene		OE/+ vs WT		OE/OE vs WT		OE/OE vs OE/+	
			Fold Change	Log2(FC)	Fold Change	Log2(FC)	Fold Change	Log2(FC)
Repair Schwann cell markers	*c-Jun*	transcription factor AP-1-like	1.53	0.61	4.50	2.17	2.79	1.48
	shh	sonic hedgehog	5.21	2.38	20.25	4.34	2.93	1.55
	Gdnf	glial cell line derived neurotrophic factor	1.82	0.86	55.72	5.8	19.97	4.32
	Bdnf	brain derived neurotrophic factor	0.77	-0.37	3.66	1.87	3.78	1.92
	Olig1	oligodendrocyte transcription factor 1	1.24	0.31	47.50	5.57	26.35	4.72
Myelin proteins	*Mpz*	myelin protein zero	0.65	-0.62	0.14	-2.81	0.22	-2.16
	Mbp	myelin basic protein	0.75	-0.41	0.13	-2.9	0.18	-2.47
	Pmp22	peripheral myelin protein 22	0.95	-0.07	0.19	-2.39	0.20	-2.34
Transcriptional Factors	*Krox20*	early growth response 2	0.96	-0.06	0.80	-0.33	0.83	-0.27
	Id2	inhibitor of DNA binding 2	2.11	1.08	9.58	3.26	4.29	2.10
	Sox2	SRY (sex determining region Y)-box 2	1.48	0.57	7.62	2.93	4.86	2.28
	Sox10	SRY (sex determining region Y)-box 10	0.58	-0.78	0.75	-0.41	1.35	0.43
	Runx2	runt related transcription factor 2	1.56	0.64	19.70	4.3	11.71	3.55

A

OE/+ vs WT			
Gene		Fold Change	log2(FC)
Gadl1	Glutamate Decarboxylase Like 1	7.31	2.87
Shh	sonic hedgehog	5.21	2.38
Slc8a3	Solute carrier family 8 member A3	4.47	2.16
Krt17	keratin 17	4.32	2.11
Pld5	phospholipase D family member 5	4.03	2.01
Tubb3	Tubulin beta 3 class III	3.73	1.9
Tenm1	teneurin transmembrane protein 1	3.73	1.9
Rps6ka6	ribosomal protein S6 kinase A6	3.53	1.82
Btc	betacellulin	3.48	1.8
Cwh43	cell wall biogenesis 43 C-terminal	3.29	1.72
Crlf1	cytokine receptor like factor 1	3.29	1.72
Mgarp	mitochondira localised glutamic acid rich protein	3.14	1.65
Neurl1a	neuralised E3 ubiquitin protein ligase 1A	3.10	1.63
Tnfrsf12a	TNF receptor superfamily member 12A	2.97	1.57
Pcdhac2	protocadherin alpha subfamily C,2	2.87	1.52
Grik3	glutamate ionotropic receptor kainate type subunit 3	0.20	-2.29
Ttll6	tubulin tyrosine ligase-like family, member 6	0.23	-2.15
Lect1	leukocyte cell derived chemotaxin 1	0.26	-1.97
Tmem28	transmembrane protein 28	0.30	-1.74
Dpysl5	dihydropyrimidinase like 5	0.31	-1.67
Fabp7	fatty acid binding protein 7	0.33	-1.62
Crygs	crystallin gamma S	0.33	-1.61
Calcoco2	calcium binding and coiled-coil domain 2	0.33	-1.6
Flt4	fms related tyrosine kinase 4	0.34	-1.57
Crybb1	crystallin beta B1	0.34	-1.54
Spock3	SPARC/osteonectin, cwcv and kazal like domains proteoglycan 3	0.35	-1.51
Cdh3	cadherin 3	0.36	-1.48
Camk4	calcium/calmodulin-dependent protein kinase IV	0.37	-1.44
Syt1	Synaptotagmin 1	0.37	-1.43
Slc1a2	solute carrier family 1 member 2	0.38	-1.41

B

OE/OE vs WT			
Gene		Fold Change	log2(FC)
Fgf5	fibroblast growth factor 5	233.94	7.87
Ucn2	urocortin 2	98.36	6.62
Btc	betacellulin	89.88	6.49
Klk9	kallikrein related peptidase 9	88.65	6.47
Prkg2	protein kinase, cGMP-dependent, type II	87.43	6.45
Pkp1	plakophilin 1	77.17	6.27
Slc17a8	solute carrier family 17 member 8	77.17	6.27
Gria1	glutamate receptor, ionotropic, AMPA1 (alpha 1)	57.68	5.85
Tnc	tenascin C	57.68	5.85
Gdnf	glial cell line derived neurotrophic factor	55.72	5.8
Kcnk10	potassium two pore domain channel subfamily K member 10	50.21	5.65
Npy5r	neuropeptide Y receptor Y5	49.87	5.64
Olig1	oligodendrocyte transcription factor 1	47.50	5.57
Nphs2	nephrosis 2, podocin	46.21	5.53
Nppb	natriuretic peptide B	45.57	5.51
Cyp2j13	cytochrome P450, family 2, subfamily j, polypeptide 13	0.01	-6.19
Plk5	polo like kinase 5	0.02	-6.05
Ttll6	tubulin tyrosine ligase-like family, member 6	0.02	-5.56
Dpysl5	dihydropyrimidinase like 5	0.02	-5.49
Etnppl	ethanolamine phosphate phospholyase	0.03	-5.27
Cyp4f14	cytochrome P450, family 4, subfamily f, polypeptide 14	0.03	-5.14
Myrfl	myelin regulatory factor-like	0.03	-5.04
Mmd2	monocyte to macrophage differentiation-associated 2	0.03	-4.86
Calcoco2	calcium binding and coiled-coil domain 2	0.04	-4.83
Clvs1	clavesin 1	0.04	-4.64
Grid2	glutamate receptor, ionotropic, delta 2	0.04	-4.61
Pla2g5	phospholipase A2, group V	0.04	-4.6
Lect1	leukocyte cell derived chemotaxin 1	0.04	-4.58
Slc6a15	solute carrier family 6 (neurotransmitter transporter), member 15	0.05	-4.42
Spock3	sparc/osteonectin, cwcv and kazal-like domains proteoglycan 3	0.05	-4.41

C

OE/OE vs OE/+			
Gene		Fold Change	log2(FC)
Ptpn5	protein tyrosine phosphatase, non-receptor type 5	98.36	6.62
Prkg2	protein kinase, cGMP-dependent, type II	72.50	6.18
Cdh22	cadherin 22	56.10	5.81
Ereg	epiregulin	48.50	5.60
Cacng3	calcium channel, voltage-dependent, gamma subunit 3	40.50	5.34
Gria1	glutamate receptor, ionotropic, AMPA1 (alpha 1)	38.85	5.28
Gpr83	G protein-coupled receptor 83	36.76	5.20
Retnlg	resistin like gamma	34.30	5.10
Pkp1	plakophilin 1	33.59	5.07
Klk9	kallikrein related-peptidase 9	32.45	5.02
Slc17a8	solute carrier family 17 member 8	28.84	4.85
Podnl1	podocan-like 1	26.91	4.75
Olig1	oligodendrocyte transcription factor 1	26.35	4.72
Rorb	RAR-related orphan receptor beta	25.28	4.66
Col25a1	collagen, type XXV, alpha 1	25.11	4.65
Plk5	polo like kinase 5	0.04	-4.63
Mmd2	monocyte to macrophage differentiation-associated 2	0.04	-4.54
Myrfl	myelin regulatory factor-like	0.06	-4.03
Bfsp2	beaded filament structural protein 2, phakinin	0.08	-3.65
B3gnt5	UDP-GlcNAc:betaGal beta-1,3-N-acetylglucosaminyltransferase	0.08	-3.64
Car14	carbonic anhydrase 14	0.08	-3.61
Dpysl5	dihydropyrimidinase-like 5	0.08	-3.58
St8sia5	ST8 alpha-N-acetyl-neuraminide alpha-2,8-sialyltransferase 5	0.08	-3.56
Cyp4f14	cytochrome P450, family 4, subfamily f, polypeptide 14	0.08	-3.56
Tmem229a	transmembrane protein 229A	0.09	-3.45
Etnppl	ethanolamine phosphate phospholyase	0.09	-3.44
Kcnj12	potassium inwardly-rectifying channel, subfamily J, member 12	0.09	-3.40
Krt17	keratin 17	0.10	-3.38
Slc36a1os	solute carrier family 36 member 1, opposite strand	0.10	-3.31
Spint1	serine protease inhibitor, Kunitz type 1	0.11	-3.24

D

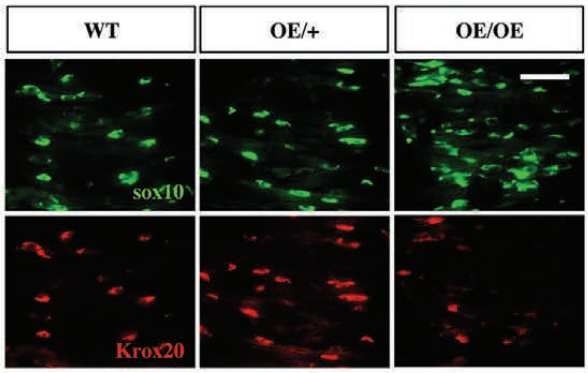

E

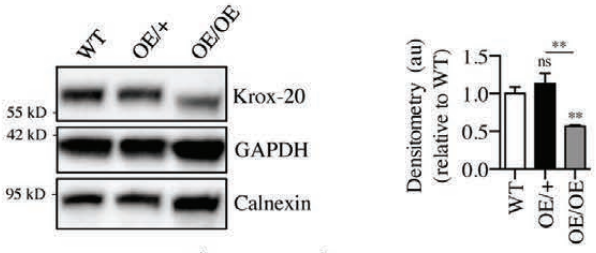

F